

Formation of Schottky Defects at the Surface of MgO, TiO₂, and SnO₂: A Comparative Density Functional Theoretical Study

M. Ménétrey, A. Markovits, and C. Minot*

Laboratoire de Chimie Théorique, Université P. et M. Curie, 4 Place Jussieu case 137,
75252 Paris Cedex 05, France

G. Pacchioni

Dipartimento di Scienza dei Materiali, Università di Milano-Bicocca, Via R. Cozzi, 53-20125 Milano, Italy

Received: April 6, 2004; In Final Form: June 23, 2004

We have performed density functional theory—generalized gradient approximation periodic calculations to study the formation of an oxygen vacancy on rutile-TiO₂(110), rutile-SnO₂(110), and MgO(100) surfaces assuming that the removed O atom remains adsorbed in the neighborhood of the vacancy (surface Schottky defect). The readsorption of the removed O atom considerably reduces the energetic cost of formation of the vacancy. The readsorption process differs from adsorption of atomic oxygen on a nondefective surface. In fact, on a regular surface an O atom binds to an oxide anion and forms a peroxy group, while on a reduced surface the O atom adsorbs preferentially on the metal cation. The study accounts also for the possible formation of formally charged defects (e.g., the F⁺ center) at the surface of ionic oxides.

1. Introduction

It is well-known that the surface reactivity is not the same when the surface is regular (stoichiometric) or reduced (substoichiometric).^{1–3} As a general rule, the most favorable adsorption modes on a perfect surface preserve the electronic gap of the oxide and can be understood in terms of acid–base reaction mechanisms; on the contrary, the adsorption on a reduced surface implies a redox mechanism in order to restore the gap that is decreased or has disappeared by effect of the reduction. Adsorption on surfaces with O vacancies belongs to the second category.

The formation of O vacancies implies an energy cost that is decreased when the removed O atom is readsorbed nearby; the atomic adsorption partially compensates the cost of formation of the defect. This paper is devoted to the study of this compensation. We investigate the thermodynamic aspects of the migration of an O atom and search for the configuration of lowest energy which includes a vacancy and an adatom on a perfect terrace. When defective surfaces are artificially prepared (under ultrahigh vacuum conditions by impact with Ar⁺ ions, for instance), the treatment may irretrievably remove O atoms.⁴ On the contrary, for smoother conditions (natural oxides or mild conditions of preparing the defective surface) the readsorption of the O atom is more likely. Defects induced in MgO by neutron irradiation are largely the result of atom displacements⁵ and the crystal, though stoichiometric, is disordered.⁶

In general, one considers the two events (desorption and readsorption of O) as independent. However, as stated above, this is not true. One reason is that an electrostatic interaction can be established between the adsorbed O atom and the vacancy, in particular if the O atom remains in the vicinity of the defect. The other reason is that the O readsorption occurs on a reduced surface instead of a perfect one, and the characteristics of the interaction can differ substantially.

Of course, the search for the best adsorption mode of an oxygen atom in the presence of a vacancy requires the obvious restriction that the adsorption does not occur on the vacancy,

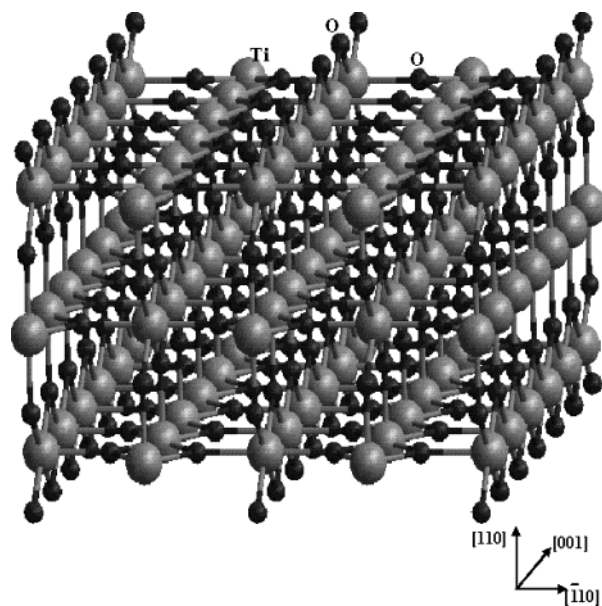


Figure 1. Perspective view of the rutile(110) slab. Metal atoms are represented by large circles and O atoms by small ones.

recreating the perfect system; the defective site remains the most reactive one^{7,8} but here we are interested in the metastable state corresponding to the displacement of an O atom from a regular lattice site to another adsorption site on the surface.

The abstraction of an oxygen atom from rutile-TiO₂(110) and rutile-SnO₂(110) (Figure 1) surfaces generates preferentially a hole in the row of bridging O atoms⁹ (Figure 2). In the following we denote the oxygen vacancy in TiO₂ and SnO₂ as V_O to distinguish it from the same defect in ionic oxides, the F centers. For TiO₂(110) the cost of the process, defined as MO₂ → MO_{2-x} + O(3P), is 4.8–7.3 eV according to embedded cluster calculations,¹⁰ 5.6–7.1 eV from periodic calculations at various coverage,¹¹ and 5.55 eV using the VASP program;¹² for SnO₂(110) it is 4.9–6.6 eV.^{13–15} (We used the experimental O₂

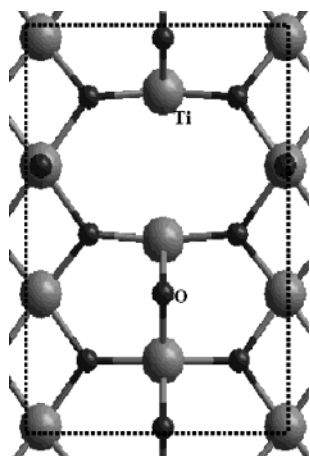


Figure 2. Top view of the unit cell of the defective rutile(110) surface at $\theta = 1/3$. Metal atoms are represented by large circles and O atoms by small ones.

dissociation energy (5.17 eV) to convert the energy of formation of the vacancy referred to $(1/2)\text{O}_2$ to that relative to the O (^3P) atom.) Formally, there is a reduction of two surface metal atoms per oxygen vacancy created: $2\text{M}^{4+} + 2\text{e}^- \rightarrow 2\text{M}^{3+}$. The electrons occupy the crystalline orbitals at the bottom of the conduction band;¹¹ these orbitals are mainly localized on the two metal cations close to the vacancy but with partial delocalization on the other cations. According to our calculations, in the case of TiO₂, this yields a high spin state ($N_\alpha - N_\beta = 2$ per oxygen vacancy), while in the case of SnO₂, the electronic ground state is closed shell.¹² The readsorption of an oxygen atom on the reduced surface can be accompanied by a redox mechanism restoring the gap: all the Ti atoms return to be Ti^{4+} and donate two electrons to the adsorbed O atom which, formally, becomes negatively charged, O^{2-} . Of course, the real charge is far from the nominal value of -2 , since TiO₂ is a semicovalent oxide. For TiO₂(110), the density of states (not presented here) demonstrates a clear restoration of a gap, while for SnO₂(110) it shows the appearance of a very small gap. An indirect proof of this analysis would be the modification of the adsorption site of the O^{2-} dianion that adapts to the electron count. On the contrary, O adsorption on the perfect surface occurs by formation of a peroxo compound. Adding an O atom to the stoichiometric surface implies that two O atoms have the oxidation state -1 and hence are bound as O_2^{2-} ion. In an ionic structure (e.g., MgO), a complex dianion, O_2^{2-} , replaces a simple one, O^{2-} ; therefore, the adsorption should take place preferentially on the surface oxygen atoms.

The abstraction of an oxygen atom from the MgO(100) surface (Figure 3) has been investigated by several authors.^{16–27} The process costs about 9 eV¹⁶ and is more difficult than on other oxides since Mg is not a reducible atom. The abstraction of a neutral oxygen atom reduces the surface by generating a neutral F^0 center, two electrons being trapped in the cavity.^{17–23} In this respect, the electronic structure of an O vacancy in MgO, the F^0 center, or in TiO₂, V_{O} , is quite different. Defects corresponding to a less drastic reduction have also been investigated. These defects are charged: the F^+ center, where only one electron is trapped in the cavity,^{24–27} has a positive charge compensating the withdrawal of an O^- ion. The formation of an empty hole, F^{2+} center, corresponds to the removal of an O^{2-} ion but is much more expensive in energy. F^{2+} centers have been proposed as diamagnetic precursors of the paramagnetic F^+ centers; however, the removal of a charged dianion has to be compensated in some way to maintain electroneutrality.²⁸

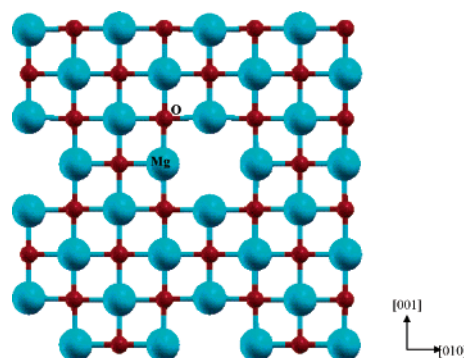


Figure 3. Top view of the surface layer of the defective MgO(100) surface. Mg atoms are represented by large circles and O atoms by small ones. The Mg atoms of the second layer are at the center of the vacancy, F^0 center.

It is important to note that the “compensation” can modify the nature of the defect. On TiO₂(110) and SnO₂(110) surfaces, the O readsorption is an oxidative process which can restore the highest oxidation state of the unsaturated metal atoms ($2\text{Ti}^{3+} \rightarrow 2\text{Ti}^{4+} + 2\text{e}^-$); the impurity states at the bottom of the conduction band due to Ti^{3+} disappear. For MgO, a formal reoxidation by O adsorption could generate in principle an F^{2+} center and an O^{2-} ion. However, the energy gain is expected to be small for two main reasons: (i) MgO is an insulator and thus a less reactive oxide than a semiconducting one; the levels of the frontier crystal orbitals (bottom of the conduction band) are less available for charge transfer. (ii) The O adatom is poorly coordinated compared to the other O atoms of the lattice and thus should be unable to accommodate extra electronic charge. This implies that there is a possible competition between the two sites, vacancy and adsorbed O atom, to accommodate the two electrons.

This paper is devoted to the study of the formation of compensated defects, formed via a Schottky process. We stress the energetic and the electronic count associated to the creation of a surface Schottky defect. After the Introduction, in sections 2 and 3 we describe the computational methods and the surface models. We present in the first part of section 4 different systems that could result from the interaction of O with the perfect or defective metal oxide surfaces. We comment on the relative trends for the different surfaces in the second part of section 4. Finally, the last section summarizes our conclusions.

2. Computational Details

We have performed periodic calculations using the VASP program,^{29–31} a plane wave basis set (kinetic energy cutoff at 396 eV), and ultrasoft pseudopotentials^{32,33} for the electron–ion interactions. Spin-polarized calculations have been done using the generalized gradient approximation with the Perdew–Wang functional.³⁴ The atoms within the supercell are relaxed until the energy difference between two subsequent steps is smaller than 0.001 eV. The calculations have been performed sampling the Brillouin zone in a $5 \times 5 \times 1$ Monkhorst–Pack set. The formation energy of an oxygen vacancy has been determined with respect to the energy of an O(^3P) atom computed at the spin-polarized level using an asymmetric box of $10 \times 11 \times 12 \text{ \AA}^3$.

3. Models of TiO₂(110), SnO₂(110), and MgO(100) Surfaces

The calculations are periodic in the three dimensions. The repetition vector perpendicular to the surface is large enough to prevent any interaction between successive slabs (the width

of the vacuum between them is >7.5 Å). The oxygen vacancy and the adsorption or readsorption are done on a single face of the slab.

For the $\text{TiO}_2(110)$ and $\text{SnO}_2(110)$ slabs we used a 1×3 unit cell and a nine atomic layer slab (three stoichiometric layers), the three top atomic layers being optimized and the others being maintained at the bulk positions. For $\text{TiO}_2(110)$, the relaxation of the bridging O is smaller than found experimentally. The distance to the layer of 6-fold coordinated Ti atoms is reduced from 1.25 to 1.09 Å instead of 0.87 Å as found experimentally.³⁵ This discrepancy has been found also in other calculations and has been attributed to soft surface phonons.^{36–38} The interlayer spacing between the layer containing the six-coordinated Ti cations, Ti_{6c} layer, (moved upward) and the Ti_{5c} layer (moved into the surface) is 0.31 vs 0.28 Å (experimental). For $\text{SnO}_2(110)$, the interlayer spacing of the bridging oxygen to the layer of 6-fold coordinated Sn_{6c} atoms is reduced from 1.29 to 1.21 Å. The interlayer spacing between the Sn_{6c} layer (moved upward) and the Sn_{5c} layer (moved into the surface) is 0.26 Å. A discussion on the effect of relaxation on $\text{SnO}_2(110)$ with Sn in different oxidation states may be found in refs 13, 15, 39, and 40. We have found that the $\text{SnO}_2(110)$ surface relaxation and the $\text{TiO}_2(110)$ surface relaxation give the same energy stabilization of 1.91–1.92 eV.

For $\text{MgO}(100)$, we have used a three-layer slab. The unit cell, $2\sqrt{2} \times 2\sqrt{2}$, contains eight MgO units per layer and possibly one oxygen vacancy. This supercell corresponds to defect coverage of 1/8. Relaxation is allowed only for the side on which the study is performed. We have optimized the top atomic layer (completely) and the second atomic layer (partially, restricting the optimization to the displacements perpendicular to the surface), with the last layer being fixed at the bulk position. In the case of the F^0 center we have found small motions of the Mg atoms (outward) and of the O atoms (inward) in agreement with previous cluster calculations.²¹

4. Results and Discussion

Usually O_2 does not dissociate on metal oxide surfaces unless vacancies are present.^{41–45} In this case O_2 dissociation is expected to imply an exothermic process and a small barrier. The fact that dissociation is not observed on regular oxide surfaces means that the energy for atomic adsorption referred to $\text{O}(^3\text{P})$ must be smaller than half the dissociation energy of O_2 : 5.17 eV in the experiment⁴⁶ (5.87 eV in our approach). Thus, atomic oxygen adsorption energies below 2.5 eV imply that the O_2 dissociation is endothermic. Assuming the same adsorption strength on a perfect and defective surface (which, however, is not exact), this value corresponds also to the largest that we can expect to reduce the cost of the vacancy formation.

As mentioned in the Introduction, on a clean and perfect terrace, the O adsorption takes place at an O site.^{1,11,14,15,47,48} One can view the process as resulting from the need to preserve the balance between cations and anions; in this respect one replaces an O^{2-} ion by a peroxo anion, O_2^{2-} , with the same global charge. The O–O distance is then close to that of the peroxo group, 1.46 Å. For TiO_2 , this allows maintaining the band gap and the resulting system has no spin; the O_2^{2-} ion replaces a bridging O^{2-} ion in the $[001]$ rows of the (110) face¹ or a tricoordinated O^{2-} ion in the basal plane.¹¹ A similar result was found on SnO_2 .^{15,48} Of course, as we mentioned before, TiO_2 and SnO_2 are not fully ionic materials and the actual anion charge is much smaller than the nominal value of -2 .

For $\text{MgO}(100)$, the adsorption energy referred to the atom is small except when adsorption occurs on surface irregularities (low-coordinated sites) but the process is endothermic when

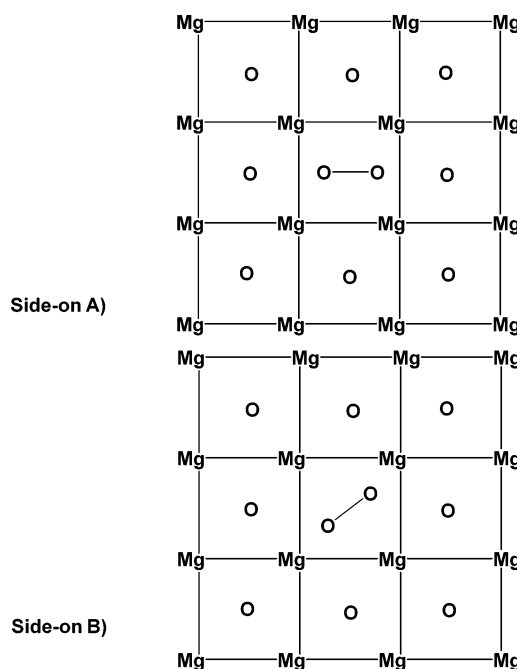


Figure 4. Orientation of the peroxo complex parallel to the $\text{MgO}(100)$ surface. Note that these adsorption modes are not the most stable ones. (side-on A) The projected O–O axis passes through the middle of two edges. (side-on B) The O–O axis is along the Mg–Mg direction.

referred to $(1/2)\text{O}_2$. Here we can expect four main adsorption modes: (i) One peroxo group, O_2^{2-} , lying parallel to the surface replaces an O^{2-} ion surrounded by four Mg ions;⁴⁷ this corresponds to the mode observed for TiO_2 and SnO_2 (but notice that in this case the steric repulsion is much smaller since the replaced O atom belongs to the bridging rows). (ii) A superoxo, O_2^- , is formed when O_2 interacts with an F center (in this case one electron of the vacancy is transferred to the adsorbed O_2 molecule).⁴⁹ (iii) An $\text{O}(^3\text{P})$ atom weakly interacts with a perfect surface. (iv) An oxygen molecule is physisorbed on the surface without interacting with the F^0 center (this situation is certainly less favorable).

(i) Peroxo Mode, O_2^{2-} . Compared with TiO_2 and SnO_2 , MgO has a much more compact surface structure and the peroxo group oriented parallel to the surface is too large to replace a single O^{2-} ion. In fact, it lies 0.88 Å above the top layer, leaving a hole in the surface plane at the position left vacant by the replaced O^{2-} ion. This corresponds to an F^{2+} center. The heat of adsorption is smaller when the O–O axis of the peroxo group is oriented in the $[010]$ direction parallel to an edge (side-on A; see Figure 4) rather than rotated by 45° in the $[110]$ direction (side-on B; see Figure 4). The perpendicular orientation (end-on geometry) allows filling the cavity and avoids the formation of an F^{2+} center, a process very expensive from the energy point of view. Indeed, the vertical peroxo group (end-on geometry) is energetically more favorable than the side-on one. With a tilt, it becomes even more stable, as found by Kantorovich and Gillan.⁴⁷ In the tilted orientation in fact it benefits from the interaction between the terminal O atom of the peroxo group and one Mg^{2+} ion of the surface; the Mg–O distance, 2.04 Å, is only slightly shorter than in the bulk, 2.1 Å. In our approach we found an adsorption energy of 2.39 eV, slightly larger than that calculated in ref 47 (2.03–2.04 eV). This is the best adsorption mode for an O atom adsorbed on the regular MgO surface (Table 1). The density of states (DOS) curve is shown in Figure 5.

(ii) $F^+ + \text{Superoxo, } \text{O}_2^-$. For the parallel orientation, the surface cavity may accommodate one electron leading to a

TABLE 1: Properties of Oxygen Atoms Adsorbed on Nondefective MgO(100), TiO₂(110), and SnO₂(110) Surfaces^a

system	adsorption site, X	adsorption mode	E_{tot} , eV	$E_{\text{ads}}(\text{O})$, eV	$E_{\text{ads}}(1/2\text{O}_2)$, eV	$r(\text{O}-\text{X})$, Å	$N_\alpha - N_\beta$
MgO	O ²⁻	peroxo parallel (A)	-284.68	0.50	-2.44	1.45	0
	O ²⁻	peroxo parallel (B)	-286.23	2.05	-0.89	1.49	0
	O ²⁻	peroxo tilted	-286.57	2.39	-0.55	1.54	0
	O ²⁻	O(³ P)	-284.83	0.65	-2.29	2.03	2
	Mg ²⁺	O(³ P)	-285.13	0.96	-1.98	2.02	2
	Mg ²⁺	O(¹ D)	-284.25	0.07	-2.86	1.96	0
TiO ₂	O ²⁻	peroxo ^b	-482.14	2.14	-0.79	1.44	0
	Ti ⁴⁺	O(³ P) ^b	-481.35	1.35	-1.59	1.71	2
SnO ₂	O ²⁻	peroxo ^b	-330.05	1.07	-1.87	1.55	0

^a E_{tot} = total energy. $E_{\text{ads}}(\text{O})$ and $E_{\text{ads}}(1/2\text{O}_2)$ are the adsorption energies referred to the free atom (-1.96 eV) and to (1/2)O₂ (-4.90 eV). $r(\text{O}-\text{X})$ is the distance of O from the nearest anion or cation on the surface. $N_\alpha - N_\beta$ is the net magnetization determined as the difference between α and β spins. The energies of the perfect slabs are -282.21 eV (MgO), -478.04 eV (TiO₂), and -327.01 eV (SnO₂). ^b Coverage $\theta = 1/3$.

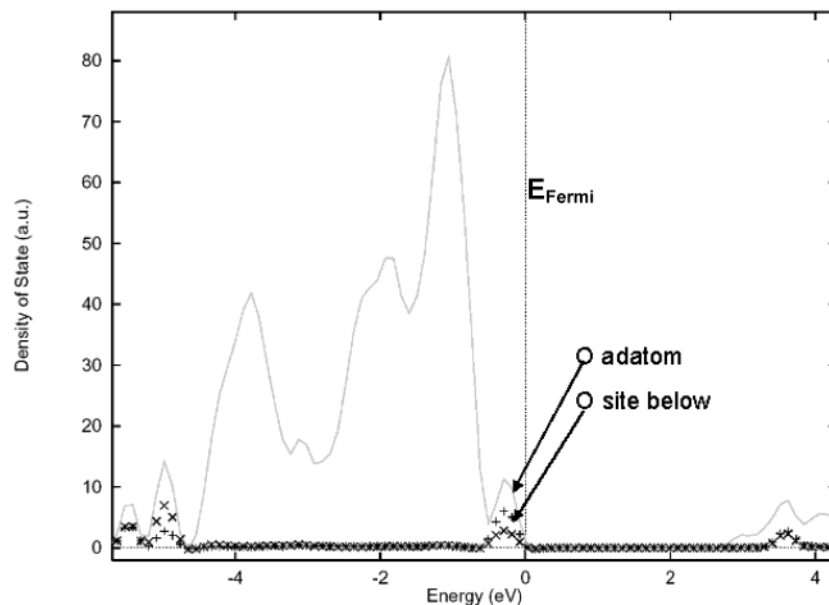


Figure 5. Density of states of an O atom adsorbed on a O²⁻ ion of a nondefective (stoichiometric) MgO surface forming a peroxo group. Solid line, total DOS; +, projection on oxygen adatom; x, projection on surface oxygen below. The charge density is shared by the two atoms from the peroxo group (at $E_F + 0.25$ eV).

superoxo, O₂⁻, adsorbed on an F⁺ center. This has been found to be more stable in energy than the peroxo (section i above), assuming a fixed orientation of the O₂⁻ molecule with the axis parallel to the surface.⁴⁹ However, our results show that relaxing the O-O distance leads to dissociation of the molecule.

(iii) O Atom (³P) on Perfect Surface. Here we consider the interaction of atomic oxygen on either a Mg²⁺ or an O²⁻ surface ion imposing a triplet state. When the adsorption is end-on, the external O (adatom) is singly coordinated and cannot bear a large negative charge; the electron density remains mostly on the O atom of the surface which benefits from the stabilizing effect of the Madelung potential. This makes the end-on orientation energetically less favorable. The interaction of an O(³P) atom with an O²⁻ ion of the surface is 0.65 eV, much smaller than for the singlet state where it is 2.39 eV (peroxo mode). For the perpendicular geometry, the O-O distance is large (2.03 Å) and the spin is almost completely localized on the adatom. The interaction of an O(³P) atom with an Mg²⁺ ion of the surface is 0.96 eV, i.e., stronger than with the O²⁻ ion (Table 1). The spin is almost entirely on the adatom with a small delocalization (0.11 e) on the nearest oxide ions of the lattice (see Figure 6).

(iv) Physisorption of O₂. The weak physisorption of a dioxygen molecule on the surface does not release enough energy to compensate the cost of the creation of a vacancy. We did not find a stable minimum for this case.

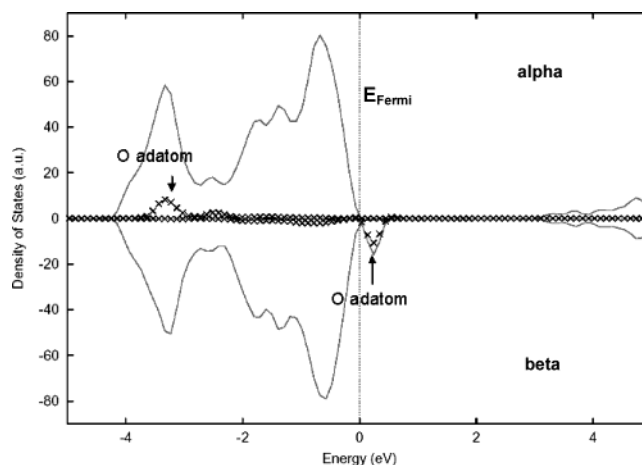


Figure 6. Density of states of an O(³P) atom adsorbed on a Mg²⁺ ion of a nondefective (stoichiometric) MgO surface. The majority spin (α) is shown by positive values and the minority spin (β) by negative values. Solid line, total DOS; x, projection on oxygen adatom. The spin is almost completely localized on the adatom (the alpha peak at $E_F - 3.5$ eV is not balanced by an occupied beta peak but by an empty one at $E_F + 0.3$ eV).

The adsorption of atomic oxygen on a reduced system is expected to be different. As mentioned in the Introduction, the adsorption of O on the reduced surfaces of TiO₂(110) and SnO₂-

TABLE 2: Properties of a Schottky Defect Formed on MgO(100), TiO₂(110), and SnO₂(110) Surfaces by Removing an O Atom from a Regular Site (Vacancy Formation) and Readsorbing It on Another Surface Site^a

system	Schottky defect ^b	E_{tot} , eV	E_1 , eV	E_2 , eV	$E_{\text{ads}}(\text{O})$, eV	$E_{\text{ads}}(1/2\text{O}_2)$, eV	$r(\text{O}-\text{X})$, Å	$N_\alpha - N_\beta$
MgO	$\text{F}_s^0 + \text{O}/\text{O}^{2-}$	-275.38	9.12	6.83	2.29	-0.65	1.53	0
	$\text{F}_s^+ + \text{O}^-/\text{O}^{2-}$	-275.35	9.12	6.86	2.26	-0.68	2.09	2
	$\text{F}_s^{2+} + \text{O}^{2-}/\text{Mg}^{2+}$	-275.39	9.12	6.83	2.29	-0.65	1.87	0
	$\text{F}_s^+ + \text{O}^-/\text{Mg}^{2+}$	-275.82	9.12	6.39	2.73	-0.21	1.94	2
TiO ₂	$\text{V}_\text{O} + \text{O}/\text{O}^{2-}$	-474.42	5.55	3.62	1.85	-1.09	1.45	2
	$\text{V}_\text{O}^{2+} + \text{O}^{2-}/\text{Ti}^{4+}$	-477.54	5.55	0.50	4.97	2.03	1.65	0
SnO ₂	$\text{V}_\text{O} + \text{O}/\text{O}^{2-}$	-322.70	5.19	4.32	0.88	-2.06	1.57	0
	$\text{V}_\text{O}^{2+} + \text{O}^{2-}/\text{Sn}^{4+}$	-324.26	5.19	2.75	2.44	-0.50	1.92	0

^a E_{tot} = total energy. E_1 is the formation energy of the vacancy referred to a free O atom. E_2 is the formation energy of the Schottky defect (creation of the vacancy and readsorption of an O atom on a different site). $E_{\text{ads}}(\text{O})$ and $E_{\text{ads}}(1/2\text{O}_2)$ are the adsorption energies referred to the free atom (-1.96 eV) and to $(1/2)\text{O}_2$ (-4.90 eV). $r(\text{O}-\text{X})$ is the distance of O from the nearest anion or cation on the surface. $N_\alpha - N_\beta$ is the net magnetization determined as the difference between α and β spins. The energies of the defective slabs are -271.13 eV (MgO), -470.53 (TiO₂), and -319.26 (SnO₂). ^b The notation $\text{V}_\text{O}^{n+} + \text{O}^{n-}/\text{X}$ refers to the species removed from the surface, O^{n-} , and the site X where it is readsorbed. V_O^{n+} represents a generic oxygen vacancy and its charge state.

(110) should take place on the metal cation because it allows maintaining an electronic gap; the adsorbed oxygen becomes formally O^{2-} and each metal atom from the surface keeps its highest oxidation number.

On reduced MgO the presence of two excess electrons in an F center allows in principle forming a new O^{2-} ion which can be adsorbed at the Mg^{2+} site. In this case the two trapped electron would be transferred to the adsorbed O atom. This could be energetically more favorable than adsorbing O at an O^{2-} site with formation of a peroxo group and leaving the electrons in the cavity (F center). However, the oxygen adatom would not be able to carry an excessive negative charge. In this case a possible compromise is that the electrons are redistributed between the O adatom and the vacancy. This would lead to a high spin system with an F^+ center and an O^- ion adsorbed on the surface, with a total of two unpaired electrons for each vacancy formed.

Results of the slab calculations for MgO, TiO₂, and SnO₂ are displayed in Tables 1 and 2. The heats of adsorption of oxygen on the perfect surfaces (Table 1) can be compared with those on the O-deficient surfaces (Table 2). Table 2 shows also the energies required for the removal of oxygen and for its readsorption. This corresponds to forming a Schottky defect at the surface of the material, and the energies reported are the formation energies of surface Schottky defects.

The O adsorption energies are always larger on the defective surface than on the perfect one. This is expected since O adsorption is an oxidative process which is more favorable when it occurs on a reduced surface. The largest $E_{\text{ads}}(\text{O})$ for all the oxides exceed 2.5 eV. The E_{ads} computed with respect to the oxygen molecule, $[(1/2)\text{O}_2]$, Table 2, is positive (indicating exothermicity) for TiO₂ and slightly negative for MgO (-0.21 eV) and SnO₂ (-0.50 eV). Note that the overestimation of the dissociation energy of O_2 in our calculations (5.87 vs 5.17 eV) renders the dissociation more difficult.

For all the defective oxides, in the presence of a vacancy, we verify that the O atom adsorbs at the metal site and remains almost exactly on top of the cation with very small deviation from the surface normal. The presence of the vacancy strongly increases the heat of adsorption on the metal cation (for TiO₂ and SnO₂ the process corresponds to an oxidation of the metal cation from a reduced state) while it does not modify significantly the heat of adsorption on the O atom. The difference in heat of adsorption for the two sites is very large for TiO₂(110) and SnO₂(110).

The adsorption energies associated with the peroxo mode and the reduction of the M^{4+} cations (leading either to two M^{3+} ions or to one M^{2+} ion) are slightly inferior to those on the

undefective surface (compare Table 1 with Table 2). For the TiO₂(110) surface, the peroxo compound corresponds to a high spin state and for SnO₂(110) surface to a low spin state.¹² The two electrons created when forming the vacancy are not involved in the bonding with the O adatom and remain localized on the metal cations. On the contrary, these electrons are responsible for the binding to the cation.

The vacancy formation energy (referred to the free atom), see E_1 in Table 2, is smaller in the case of SnO₂, 5.19 eV, than in the case of TiO₂, 5.55 eV, since Sn is more reducible than Ti. The fourth ionization potential of the two atoms is 40.72 and 43.24 eV, respectively. However, the migration energy, E_2 , defined as the cost of removing an O atom from a lattice position and readsorbing it on the defective surface, is higher in the case of SnO₂, 2.75 eV, than in the case of TiO₂, 0.50 eV, since the adsorption of atomic O on a metal cation of the substoichiometric surface, $E_{\text{ads}}(\text{O})$, is larger on TiO₂, 4.97 eV, than on SnO₂, 2.44 eV.

For MgO(100), the adsorption of O^{2-} on a metal cation, Mg^{2+} , leading to a closed shell system ($\text{F}^{2+} + \text{O}^{2-}_{\text{ads}}$), is not the lowest energy state, contrary to the findings for TiO₂(110) and SnO₂(110). A high spin state is lower in energy. This is because an O^{2-} ion cannot be stabilized by coordination to a single Mg^{2+} ion but has to be surrounded by several cations. Then, only in this case, the Madelung potential of the system is large enough to stabilize the doubly charged state. The lowest energy solution, Table 2, implies the redistribution of the two electrons between the vacancy and the O adatom (high spin state). This corresponds to an F^+ center with a singly charged ion, O^- , adsorbed on top of a Mg^{2+} surface cation. We show in Figure 7 the DOS curve and in Figure 8 the map of the spin density for this mode. The peaks for the odd electrons clearly appear in the DOS curve at $E_F - 0.25$ eV, and the map shows the presence of the spin both in the cavity and on the adatom, Figure 8. Thus, the energetically most favorable form of a surface Schottky defect in MgO corresponds to two magnetic centers on the surface. We have recently shown that the F^+ center is easily stabilized when the adatom is protonated.¹⁶ It is remarkable to see that the O migration is sufficient to provide a periodic neutral model with an F^+ center. Indeed, periodic modeling cannot easily deal with charged systems. The present model, being neutral, does not suffer from this limitation.

The adsorption of atomic oxygen at the O^{2-} site (peroxo mode) associated with the F^0 center is less favorable. The heat of adsorption, 2.29 eV in Table 2, is similar to that in the absence of defect, 2.39 eV, Table 1. Also, in this case the peroxo group is slightly tilted. Surprisingly, the high spin state (triplet) is only 0.03 eV less stable than the singlet configuration. It can be seen

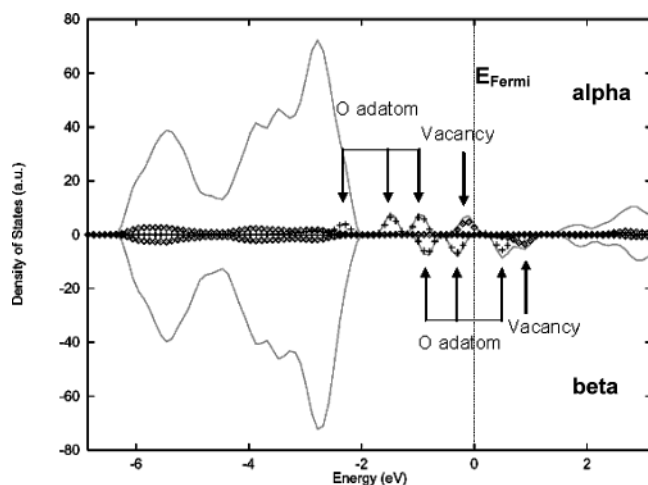


Figure 7. O[−] on Mg²⁺ for a defective MgO surface (F_s⁺). Total DOS and projection on the O adatom (+) and on the Mg atoms (◇) adjacent to the O vacancy. The alpha peak at $E_F - 0.25$ eV (◇) corresponds to the F⁺ center. The beta peak at $E_F + 0.4$ eV (+) corresponds to the missing electron of the adatom (O[−]). Eight peaks are visible, six below the Fermi level (four alpha and two beta) and two above (two beta; one of them is localized on the O adatom (+) and the other within the vacancy (◇)). Thus there are two unpaired electrons, one on the O adatom and the other within the vacancy.

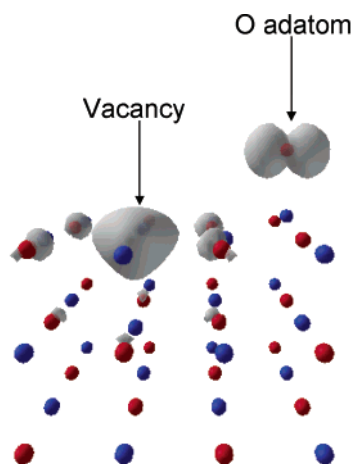


Figure 8. Spin density plot for a Schottky defect at the surface of MgO. The defect consists of an O[−] ion adsorbed on a Mg²⁺ cation near an F⁺ center. The ground state of the surface complex is triplet. The spin is predominantly localized on the O adatom and within the oxygen vacancy.

in two ways: (i) an F⁰ center with physisorption of atomic O(³P) on an O^{2−} ion of the lattice (triplet ground state of the peroxo complex), this being compatible with the long O—O distance, 2.09 Å, Table 2; (ii) an F⁺ center and an O[−] ion adsorbed on a O^{2−} ion of the surface (O/O^{2−}). This situation formally corresponds to an O₂^{3−} ion that should have a long O—O distance since the σ^*_{OO} is occupied. The DOS curve and the spin density map show that this latter structure is indeed that which forms. The highest peak of the spin-polarized part of the DOS curve is localized on the O adatom and in the vacancy (F⁺ center).

5. Conclusion

Our results show that the readsorption of the removed oxygen atom decreases the energy cost of the formation of a vacancy. At the same time, it modifies the nature of the vacancy. For TiO₂(110) and SnO₂(110), it preserves an energy gap, each metal atom bearing its highest oxidation number. In fact, the O atom

removed from the bridging rows is preferentially adsorbed on top of the metal cations, Ti_{5c} or Sn_{5c}. The compensation in energy for the readsorption is particularly large for TiO₂(110). For MgO(100), the low spin state, F²⁺ + O^{2−} on Mg²⁺, is not favorable energetically. The migration of oxygen leads to a high spin state, and the final system is an F⁺ center and O[−] adsorbed on Mg²⁺. The O migration provides a periodic neutral model with an F⁺ center. This is an alternative to the recent proposed model using a hydrogenated surface (an OH migration).¹⁶

Acknowledgment. This work has been accomplished in the framework of the GDR “Dynamique Moléculaire Quantique Appliquée à la catalyse”. Computational facilities provided by IDRIS and CCR are also acknowledged. G.P. thanks the “Centre français pour l'accueil et les échanges internationaux” (EGIDE) for supporting his stay at the University of Paris VI.

References and Notes

- (1) Calatayud, M.; Markovits, A.; Minot, C. *Catal. Today* **2004**, 89/3, 269.
- (2) Calatayud, M.; Markovits, A.; Menetrey, M.; Mguig, B.; Minot, C. *Catal. Today* **2003**, 85, 125.
- (3) Menetrey, M.; Markovits, A.; Minot, C. *Surf. Sci.* **2003**, 524, 49.
- (4) Henrich, V. E. *Rep. Prog. Phys.* **1985**, 48, 1481.
- (5) Wertz, J. E.; Orton, J. W.; Auzins, P. *Discuss. Faraday Soc.* **1961**, 31, 140.
- (6) Nelson, R. L.; Tench, A. J.; Harmsworth, B. J. *Trans. Faraday Soc.* **1967**, 1427.
- (7) Yamaguchi, Y.; Nagasawa, Y.; Shimomura, S.; Tabata, K.; Susuki, E. *Chem. Phys. Lett.* **2000**, 316, 477.
- (8) Slater, B.; Catlow, C. R. A.; Williams, D. E.; Stoneham, A. M. *Chem. Commun.* **2000**, 1235.
- (9) Diebold, U. *Surf. Sci. Rep.* **2003**, 48, 53.
- (10) Bredow, T.; Pacchioni, G. *Chem. Phys. Lett.* **2002**, 355, 417.
- (11) Rasmussen, M. D.; Molina, L. M.; Hammer, B. *J. Chem. Phys.* **2004**, 120, 988.
- (12) Bouzoubaa, A.; Markovits, A.; Calatayud, M.; Minot, C. Submitted to *Catal. Today*.
- (13) Oviedo, J.; Gillan, M. J. *Surf. Sci.* **2000**, 467.
- (14) Sensato, F. R.; Custodio, R.; Calatayud, M.; Beltran, A.; Andres, J.; Sambrano, J. R.; Longo, E. *Surf. Sci.* **2002**, 511, 408.
- (15) Sensato, F. R.; Treu-Filho, O.; Longo, E.; Sambrano, J. R.; Andres, J. *J. Mol. Struct. (THEOCHEM)* **2001**, 541, 69.
- (16) Ménétrey, M.; Markovits, A.; Minot, C.; Vitto, A. D.; Pacchioni, G. *Surf. Sci.* **2004**, 549, 294.
- (17) Tench, A. J.; Nelson, R. L. *J. Colloid Interface Sci.* **1968**, 26, 364.
- (18) Tench, A. J. *Surf. Sci.* **1971**, 25, 625.
- (19) Kantorovich, L. N.; Holender, J. M.; Gillan, M. J. *Surf. Sci.* **1995**, 343, 221.
- (20) Castanier, E.; Noguera, C. *Surf. Sci.* **1996**, 364, 1.
- (21) Ferrari, A. M.; Pacchioni, G. *J. Phys. Chem.* **1995**, 99, 17010.
- (22) Scorza, E.; Birkenheuer, U.; Pisani, C. *J. Chem. Phys.* **1997**, 107, 9645.
- (23) Nasluzov, V. A.; Rivanenkov, V. V.; Gordienko, A. B.; Neyman, K. M.; Birkenheuer, U.; Rösch, N. *J. Chem. Phys.* **2001**, 115, 8157.
- (24) Kramer, J.; Ernst, W.; Tegenkamp, C.; Pfnür, H. *Surf. Sci.* **2002**, 517, 87.
- (25) Kramer, J.; Tegenkamp, C.; Pfnür, H. *Phys. Rev. B* **2003**, 67, 235401.
- (26) Illas, F.; Pacchioni, G. *J. Chem. Phys.* **1998**, 108, 7835.
- (27) Sousa, C.; Pacchioni, G.; Illas, F. *Surf. Sci.* **1999**, 429, 217.
- (28) Chiesa, M.; Paganini, M. C.; Giamello, E.; Valentin, C. D.; Pacchioni, G. *Angew. Chem., Int. Ed.* **2003**, 42, 1759.
- (29) Kresse, G.; Hafner, J. *Phys. Rev. B* **1993**, 47, 558.
- (30) Kresse, G.; Hafner, J. *Phys. Rev. B* **1993**, 48, 13115.
- (31) Kresse, G.; Hafner, J. *Phys. Rev. B* **1994**, 49, 14251.
- (32) Vanderbilt, D. *Phys. Rev. B* **1990**, 41, 7892.
- (33) Kresse, G.; Hafner, J. *J. Phys.: Condens. Matter* **1994**, 6, 8245.
- (34) Perdew, J. P.; Wang, Y. *Phys. Rev. B* **1992**, 45, 13244.
- (35) Charlton, G.; Howes, P. B.; Nicklin, C. L.; Steadman, P.; Taylor, J. S. G.; Muryn, C. A.; Harte, S. P.; Mercer, J.; McGrath, R.; Norman, D.; Turner, T. S.; Thornton, G. *Phys. Rev. Lett.* **1997**, 78, 495.
- (36) Bates, S. P.; Kresse, G.; Gillan, M. J. *Surf. Sci.* **1997**, 385, 386.
- (37) Albaret, T.; Finocchi, F.; Noguera, C. *Faraday Discuss.* **1999**, 114, 285.
- (38) Reuter, K.; Scheffler, M. *Phys. Rev. B* **2001**, 65, 355406.

- (39) Goniakowski, J.; Holander, J. M.; Kantorovich, L. N.; Gillan, M. J.; White, J. A. *Phys. Rev. B* **1996**, *53*, 957.
- (40) Manassidis, I.; Goniakowski, J.; Kantorovich, L. N.; Gillan, M. J. *Surf. Sci.* **1995**, *339*, 258.
- (41) Onishi, H.; Egawa, C.; Aruga, T.; Iwasawa, Y. *Surf. Sci.* **1987**, *191*, 479.
- (42) Henderson, M. A.; Epling, W. S.; Perkins, C. L.; Peden, C. H. F.; Diebold, U. *J. Phys. Chem. B* **1999**, *103*, 5328.
- (43) Lu, G.; Linsebigler, A.; Yates, J. T., Jr. *J. Chem. Phys.* **1995**, *102*, 3005.
- (44) Lu, G.; Linsebigler, A.; Yates, J. T., Jr. *J. Chem. Phys.* **1995**, *102*, 4657.
- (45) Rusu, C. N.; Yates, J. T., Jr. *Langmuir* **1997**, *13*, 4311.
- (46) *Handbook of Chemistry and Physics*, 58th ed.; CRC Press: Cleveland, 1977.
- (47) Kantorovich, L.; Gillan, M. *Surf. Sci.* **1997**, *374*, 373.
- (48) Beltrán, A.; Sembrano, J. R.; Calatayud, M.; Sensato, F. R.; Andres, J. *Surf. Sci.* **2001**, *490*, 116.
- (49) Pacchioni, G.; Ferrari, A. M.; Giamello, E. *Chem. Phys. Lett.* **1996**, *255*, 58.